T1 Mapping of the Prostate Using Single-Shot T1FLASH

A Clinical Feasibility Study to Optimize Prostate Cancer Assessment

Al-Bourini, Omar MD[*]; Seif Amir Hosseini, Ali MD, MSc[*]; Giganti, Francesco MD, PhD[†,‡]; Balz, Julia[*]; Heitz, Luisa Gerda[*]; Voit, Dirk PhD[§]; Lotz, Joachim MD[*,‖]; Trojan, Lutz MD[¶]; Frahm, Jens PhD[§]; Uhlig, Annemarie MD, MPH[¶]; Uhlig, Johannes MD, MPH[*]

Abstract

Purpose

The aim of this study was to assess the clinical feasibility of magnetic resonance imaging (MRI) T1 mappingusing T1FLASH for assessment of prostate lesions.

Methods

Participants with clinical suspicion for prostate cancer (PCa) were prospectively enrolled between October 2021 and April 2022 with multiparametric prostate MRI (mpMRI) acquired on a 3 T scanner. In addition, T1 mapping was accomplished using a single-shot T1FLASH technique with inversion recovery, radial undersampling, and iterative reconstruction. Regions of interest (ROIs) were manually placed on radiologically identified prostate lesions and representative reference regions of the transitional zone (TZ), benign prostate hyperplasia nodules, and peripheral zone (PZ). Mean T1 relaxation times and apparent diffusion coefficient (ADC) values (b = 50/b = 1400 s/mm^2) were measured for each ROI. Participants were included in the study if they underwent ultrasound/MRI fusion-guided prostate biopsy for radiologically or clinically suspected PCa. Histological evaluation of biopsy cores served as reference standard, with grading of PCa according to the International Society of Urological Pathology (ISUP). ISUP grades 2 and above were considered clinically significant PCa for the scope of this study. Histological results of prostate biopsy cores were anatomically mapped to corresponding mpMRI ROIs using biopsy plans. T1 relaxation times and ADC values were compared across prostate regions and ISUP groups. Across different strata, T1 relaxation time, ADC values, and diagnostic accuracy (area under the curve [AUC]) were compared using statistical methods accounting for clustered data.

Results

Of 67 eligible participants, a total of 40 participants undergoing ultrasound/MRI fusion-guided prostate biopsy were included. Multislice T1 mapping was successfully performed in all participants at a median acquisition time of 2:10 minutes without evident image artifacts. A total of 71 prostate lesions was radiologically identified (TZ 49; PZ 22). Among those, 22 were histologically diagnosed with PCa (ISUP groups 1/2/3/4 in n = 3/15/3/1 cases, respectively). In the TZ, T1 relaxation time was statistically significantly lower for PCa compared with reference regions (P = 0.029) and benign prostate hyperplasia nodules (P < 0.001). Similarly, in the PZ, PCa demonstrated shorter T1 relaxation times versus reference regions (P < 0.001). PCa also showed a trend toward shorter T1 relaxation times (median, 1.40 seconds) compared with radiologically suspicious lesions with benign histology (median, 1.47 seconds), although statistical significance was not reached (P = 0.066). For discrimination of PCa from reference regions and benign prostate lesions, T1 relaxation times and ADC values demonstrated AUC = 0.80 and AUC = 0.83, respectively (P = 0.519). Discriminating PCa from radiologically suspicious lesions with benign histology, T1 relaxation times and ADC values showed AUC = 0.69 and AUC = 0.62, respectively (P = 0.446).

Conclusions

T1FLASH-based T1 mapping yields robust results for quantification of prostate T1 relaxation time at a short examination time of 2:10 minutes without evident image artifacts. Associated T1 relaxation times could aid in discrimination of significant and nonsignificant PCa. Further studies are warranted to confirm these results in a larger patient cohort, to assess the additional benefit of T1FLASH maps in conjunction with mpMRI sequences in the setting of deep learning, and to evaluate the robustness of T1FLASH maps compared with potentially artifact-prone diffusion-weighted imaging sequences.

INTRODUCTION

Prostate cancer (PCa) is the second most common malignancy in men, accounting for 7.1% of worldwide incident cancer cases in 2018.[1] Autopsy studies have demonstrated that, among men dying of other causes, the prevalence of so-called clinically nonsignificant PCa (nsPCa) ranged from 5% at age <30 years to 59% at age >79 years.[2] In contrast, it is crucial to accurately identify clinically significant PCa (csPCa) that could result in death. The exact clinical definition of significant PCa is difficult and varies in the literature. Commonly, the International Society of Urological Pathology (ISUP) grading system is used, with ISUP group ≥2 PCa designated as significant PCa.[3]

Magnetic resonance imaging (MRI) is the radiological mainstay for comprehensive evaluation of the prostate, which is reported using the Prostate Imaging Reporting and Data System (PI-RADS) in its most recent version 2.1.[4] The 5-point PI-RADS Likert scale quantifies the radiological probability of csPCa. In a Cochrane review evaluating the diagnostic performance of multiparametric prostate MRI (mpMRI), pooled sensitivity and specificity were 0.91 (95% CI, 0.83–0.95) and 0.37 (95% CI, 0.29–0.46) for ISUP ≥2 PCa.[5] Although the clinical utility of mpMRI is undoubted, its moderate specificity could result in false-positive findings. Moreover, the capability of mpMRI to discriminate between different PCa ISUP groups is suboptimal, thus complicating image-based PCa risk assessment and active surveillance.[6]

To address these limitations, novel MRI techniques have been developed in recent years. For example, there have been efforts to optimize T2-weighted imaging or diffusion-weighted imaging (DWI) as well as assessment of prostate MRI using deep learning.[7–10]

Another approach is the evaluation of spin-lattice (T1) relaxation time through so-called T1 mapping, which provides reproducible data on tissue properties.[11] Specifically, T1 relaxation times have been demonstrated to correlate with the extracellular volume of evaluated tissue.[12] T1 mapping is routinely used in cardiac MRIfor detection and quantification of myocardial scars, combining information from T1 maps acquired before and after intravenous administration of gadolinium-based contrast media with patients' hematocrit.[11] Still, only few studies have evaluated its utility for prostate assessment with varying techniques and results. For example, Baur et al used a modified Look-Locker inversion recovery (MOLLI) T1 mapping MRI sequence to assess 23 PCa patients, whereas Foltz et al used magnetization-prepared spiral imaging to assess T1 relaxation times in 13 PCa patients.[13,14] However, these studies are limited by small patient cohorts and a time-consuming T1 map acquisition.

A novel approach to T1 mapping (T1FLASH) relies on a fast low-angle shot (FLASH) readout of a single inversion recovery process, which has been described earlier.[15,16] The technique exploits radial undersampling for spoiled FLASH acquisitions in combination with nonlinear inverse reconstruction of serial images and pixelwise fitting of T1 values. It allows for robust and rapid T1 mapping within a few seconds and offers high spatial resolution, as well as

accurate and precise T1 relaxation time measurements as evaluated using a reference phantom.[15,16]

The aims of this study were to evaluate T1FLASH for T1 mapping technique of prostate lesions and to compare its accuracy in PCa assessment to ADC values.

MATERIALS AND METHODS

This prospective study included participants with clinical suspicion for PCa (ie, elevated PSA levels, short PSA level doubling time, prostate lesions detected on transrectal ultrasound [US], or suspicious digital rectal examination) scheduled for mpMRI at a tertiary referral center in central Germany from October 2021 to April 2022. Exclusion criteria were general MRI contraindications and age <18 years. Eligible participants were informed about study participation before study enrollment and provided written informed consent. Only participants who subsequently underwent prostate biopsy or resection with histological assessment of prostate lesions were included in the final analyses.

This study received prior approval by the local ethics committee (ID 21/4/19), was prospectively registered at the German Clinical Trials Register (ID DRKS00018062), and was conducted according to the most recent version of the Declaration of Helsinki.

MRI Acquisition

All examinations were performed on a 3 T MRI scanner (Magnetom VIDA; Siemens Healthineers, Erlangen, Germany) using suitable elements of the spine and abdominal coil. The standardized prostate mpMRI protocol included a transversal T1-weighted turbo spin echo sequence, triplanar T2-weighted turbo spin echo sequences, transversal echo planar imaging DWI sequences, and dynamic contrast enhancement (DCE) sequences after bodyweight-adjusted intravenous administration of gadolinium-based contrast media (0.1 mmol gadolinium/kg body weight using gadobutrol [Gadovist; Bayer Vital GmbH, Leverkusen, Germany]), according to recommendations by current international guidelines.[17] In addition, a T1FLASH map was acquired. A full prostate MRI protocol for this study chronologically included T1-weighted, T2-weighted, T1FLASH map, DWI/ADC, and DCE sequences.

For mpMRI preparation, all participants were asked to empty their rectum before the examination. Intravenous administration of 10 mg butylscopolamin was performed immediately before the scan and before acquisition of DWI sequences (to a total dose of 20 mg butylscopolamin), respectively, to reduce artifacts related to intestinal motility. MpMRI quality was rated using the Prostate Imaging Quality (PI-QUAL) scale.[18]

Diffusion-weighted imaging parameters were set as follows: field of view, 200 × 200 mm; in-plane resolution, 1.4 × 1.4 mm; slice thickness, 3 mm (no slice gap); number of slices depending on craniocaudal prostate diameter; repetition time, 5900 milliseconds; echo time, 76 milliseconds; and measures b-values of b = 50, b = 800, and b = 1400 s/mm^2. Apparent diffusion coefficient maps were calculated based on b = 50 and b = 1400 s/mm^2 images. The median DWI acquisition time was 9:10 minutes for 30 slices. Diffusion-weighted imaging image calculation was based on the preinstalled MRI scanner software (software version XA31). Additional technical details on the mpMRI protocol are provided in the Supplemental Material, https://links.lww.com/RLI/A786.

T1 mapping was accomplished using T1FLASH.[15,16] This technique uses a single slice-selective 180-degree inversion pulse and probes the resulting inversion recovery process by a

continuous series of spoiled FLASH images with randomized radiofrequency phases.[19] The individual real-time acquisitions use a golden angle radial trajectory with pronounced undersampling of only 17 radial spokes. The T1 accuracy of T1FLASH mapping was validated using a reference phantom in an earlier study.[19] For prostate MRI, repetition time of 3.29 milliseconds, echo time of 2.09 milliseconds, and a flip angle of 6 degrees yields an individual image acquisition time of 55.9 milliseconds. The inversion recovery process was covered by a total of 63 images, which were followed by 5 acquisitions with the body coil to improve the numerical stability of the iterative reconstruction.[20] The estimation of serial images by regularized nonlinear inversion[21] was followed by denoising using a modified nonlocal means filter that avoids blurring.[22] Finally, quantitative maps of T1 relaxation times were obtained by pixelwise fitting.[15] Overall, the acquisition time for a single T1 map is only 3.80 seconds. Other parameters for prostate T1 maps were a transverse field of view of 224 × 224 mm, an in-plane resolution of 1.0 mm × 1.0 mm, and a slice thickness of 3.0 mm. T1FLASH involved a multislice recording without gaps, with the number of slices depending on the craniocaudal diameter of the prostate. Typically, the total acquisition and reconstruction time for T1 maps was 2:10 minutes for at least 30 slices. Online reconstruction, visualization, and storage of T1 maps without the need for any user interference were ensured by a dedicated GPU computer (2 XEON E5-2650 v4 CPU [Intel Corporation, Santa Clara, CA]; 128 GB RAM, 8 NVIDIA TITAN Xp GPU [NVIDIA Corporation, Santa Clara, CA]) bypassing the host of the MRI system by use of a 1 GBit link.

Radiological MRI Evaluation

Multiparametric prostate MRI studies were systematically evaluated by the same radiologist with more than 5 years of experience in prostate MRI (approximately 400 annual scans) and assessed according to PI-RADS v2.1 based on T2-weighted, DWI, and DCE sequences.[17] All prostate lesions were identified and targeted on a standardized prostate sector map.

Regions of interest (ROIs) were placed by the radiologist, delineating PIRADS 3+ prostate lesions on T2-weighted or DWI images on one representative transversal slice using the Mint lesion software (version 3.8.5; Mint Medical, Heidelberg, Germany). The ROIs were copied to the corresponding T1 maps and ADC maps. In cases of obvious misalignment (ie, patient movement), ROIs were manually corrected. For each ROI, the mean T1 relaxation time (ms) and ADC values (s/mm^2) were calculated. Additional ROIs were placed in representative reference regions of the transitional zone (TZ), benign prostate hyperplasia (BPH) nodules, and the peripheral zone (PZ) that did not yield radiologically suspicious prostate lesions (PIRADS 1 or 2). Reference regions identified with csPCa or nsPCa on systemic prostate biopsy (see below) and histological analyses were omitted from further analyses.

Prostate Biopsy and Histological Analyses

Participants with radiologically suspicious prostate lesions (PI-RADSv2.1 score ≥3) underwent combined targeted + systematic prostate biopsy using a transrectal US/MRI fusion-guided approach (BiopSeeTM System, Version 2.1; Medcom GmbH, Darmstadt, Germany). Participants without radiologically evident prostate lesions but high

suspicion of csPCa (ie, massive PSA level elevation, high PSA density, or short PSA level doubling time) underwent systematic transrectal US/MRI fusion-guided biopsy as well.

All prostate biopsy cores underwent histopathological analyses. If diagnosed with PCa, the Gleason patterns and grade groups were rated according to the recommendations of the 2014 ISUP consensus conference on Gleason grading of prostatic carcinoma.[23] For the scope of this study, ISUP group ≥2 PCa were considered csPCa. Histological analyses were anatomically mapped to corresponding ROIs on MR images defined during radiological assessment using the transrectal US/MRI fusion-guided biopsy plans. For all statistical evaluations, histopathology reports were defined as the reference standard.

Statistical Analyses

Continuous parameters are provided as median with interquartile range (IQR). Categorical variables are provided as absolute number and percent. T1 relaxation times and ADC values of PCa lesions identified on mpMRI were compared with those of reference regions in the TZ, PZ, and BPH nodules as well as radiologically suspicious lesions with benign histology. All statistical analyses were restricted to regions that were histologically assessed and anatomically mapped to corresponding mpMRI ROIs using transrectal US/MRI fusion-guided biopsy plans. Further subgroup analyses were performed according to ISUP group and compared with radiologically suspicious lesions that yielded no cancerous tissue on histological analyses.

Because of the nonnormal distribution of continuous T1 relaxation times and ADC values (assessed by the Shapiro-Wilk normality test), nonparametric tests were used for statistical analyses. As proposed by Rosner et al,[24] a specific version of the Wilcoxon rank sum test was implemented that accounted for clustered data (ie, multiple prostate lesions per patient). Overall differences in T1 relaxation time and ADC values across multiple strata were evaluated using the method proposed by Datta and Satten.[25]

The diagnostic performance of T1 relaxation time and ADC values was evaluated with the receiver operating characteristics (ROC) curve and area under the ROC curve (AUC) for discrimination of (1) PCa from reference regions in the TZ, PZ, BPH nodules, as well as radiologically suspicious prostate lesions with benign histology, and (2) PCa from radiologically suspicious prostate lesions with benign histology. AUCs of T1 relaxation time and ADC values were compared using the method proposed by Obuchowski accounting for clustered data.[26] Cutoff values for calculation of test sensitivity and specificity were defined using the Youden index.[27]

Statistical analyses were performed using R version 4.2.0 (R Core Development Team, Vienna, Austria) and RStudio version 2022.02.3+492 (RStudio Inc, Boston, MA). All provided *P* values are 2-sided. A *P* value of <0.05 was chosen to indicate statistical significance.

RESULTS

Study Cohort

A total of 67 eligible participants with median (IQR) age of 67.5 (62.2–72.5) years was screened for study inclusion and imaged with mpMRI including T1FLASH mapping. Of these, 40 participants were included in the study that underwent US/MRI fusion-guided prostate biopsy with histological examination (37/40 with PIRADS 3+; 3/40 with high clinical PCa suspicion). In the 3 patients with PIRADS 2 scores, no PCa was histologically diagnosed.

MpMRI quality was assessed as PI-QUAL 4 in 15 cases (38%) and PI-QUAL 5 in 25 cases (62%). T1 mapping was successfully performed in all participants at a median acquisition time of 2:10 minutes for a stack of 30 images without evident image artifacts. Representative cases are provided in Figures 1 and 2.

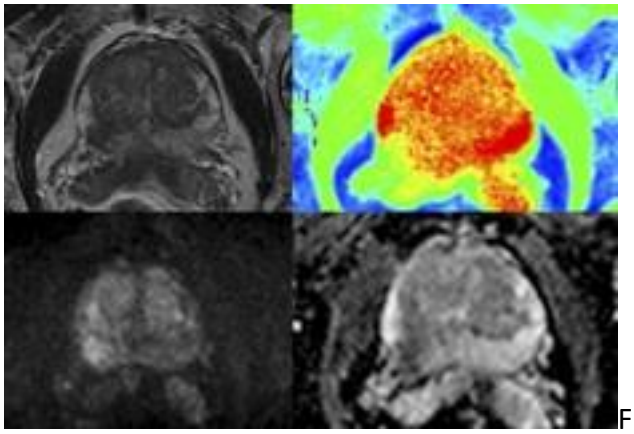
FIGURE 1:
A 77-year-old patient referred to mpMRI for clinically suspected prostate cancer. The transversal T2-weighted sequence (top left) shows a T2-weighted hypointense lesion in the right posterior peripheral zone. DWI (b = 1400, bottom left) and ADC map (bottom right) demonstrate a corresponding diffusion restriction, resulting in a PIRADSv2.1 score of 4. The T1 map shows a correlating signal abnormality (top right). Histological assessment confirmed a prostatic adenocarcinoma (Gleason 8).

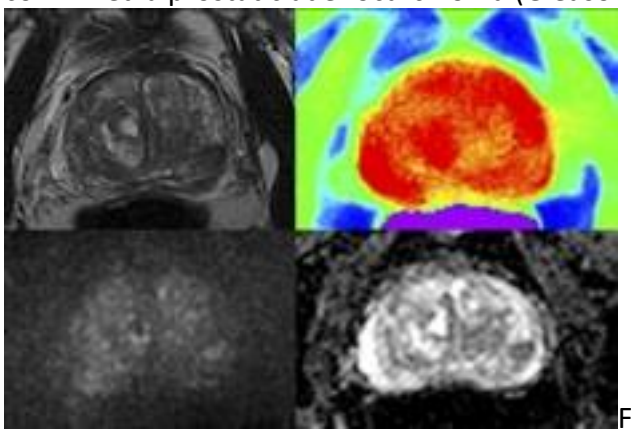
FIGURE 2:
A 68-year-old patient referred to mpMRI for clinically suspected prostate cancer. The transversal T2-weighted sequence (top left) shows a T2-weighted hypointense lesion in the left posterior peripheral zone. DWI (b = 1400, bottom left) and ADC map (bottom right)

demonstrate a corresponding diffusion restriction, resulting in a PIRADSv2.1 score of 4. The T1 map shows no correlating signal abnormalities (top right). Targeted and systemic US/MRI fusion-guided biopsies and histological assessment revealed not malignant changes.

Radiological Analyses

Among the 40 histologically assessed participants, 71 prostate lesions were radiologically identified, with a median (IQR) number of 2 (1–2) prostate lesions per patient. The prostate lesions were rated with a PIRADSv2.1 score of 2/3/4/5 in 13/12/34/12 cases, respectively. Prostate lesions were in the PZ in 22/71 (31%) cases, and in the TZ in 49/71 (69%) cases.

Histological Analyses

Of the 71 radiologically identified prostate lesions, 22 were csPCa (11 in the TZ, 11 in the PZ). On the patient level, 17/40 (42%) patients were diagnosed with PCa. The median (IQR) PCa diameter was 13.2 (10.2–18.9) mm. ISUP groups 1/2/3/4 were diagnosed in 3/15/3/1 prostate lesions, respectively. Reference regions of the TZ and PZ, as well as BPH nodules that were histologically assessed as containing no PCa were radiologically delineated in 23, 38, and 16 cases, respectively. In 1 patient, no reference regions were available due to changes after transurethral resection of the prostate.

Prostate Tissue Assessment Using T1 Mapping and ADC Values

T1 relaxation times and ADC values of prostate lesions and reference regions are provided in Table 1 and Figure 3. Using the clustered Wilcoxon rank sum test, there was a statistically significant overall difference in T1 relaxation time across prostate lesions and reference regions ($P < 0.001$). Evaluating PCa lesions in the TZ, the T1 relaxation time was statistically significantly lower compared with TZ reference regions ($P = 0.029$) and BPH nodules ($P < 0.001$). Prostate cancer lesions in the PZ demonstrated shorter T1 relaxation time versus PZ reference regions ($P < 0.001$).

TABLE 1 - T1 Relaxation Time (s) and ADC Values (s/mm^2) According to Prostate Regions

Parameter	Level	Peripheral Zone	Transitional Zone	BPH Nodule	Prostate Lesion (Benign Histology)	PCa
n		38	23	16	49	22
T1 relaxation time	Median (IQR)	1.72 (1.5–1.83)	1.49 (1.44–1.56)	1.59 (1.55–1.68)	1.47 (1.38–1.55)	1.4 (1.34–1.45)
ADC value	Median (IQR)	1.56 (1.41–1.67)	1.14 (1.09–1.23)	1.26 (1.17–1.46)	0.884 (0.799–0.965)	0.796 (0.751–0.897)

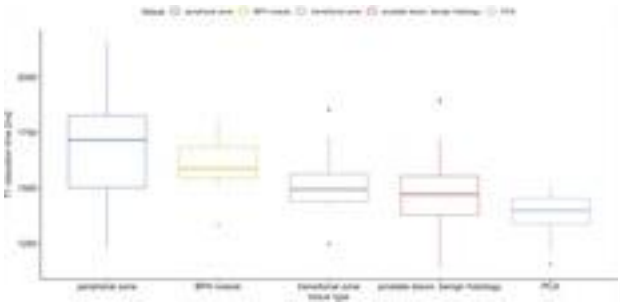

FIGURE 3:
T1 relaxation times (milliseconds) according to prostate tissue types.

T1 relaxation time and ADC values according to ISUP groups in PCa patients are summarized in Table 2 and Figure 4 on a lesion level. In general, PCa lesions showed shorter T1 relaxation times (median [IQR], 1.40 [1.38–1.45] seconds) compared with benign prostate lesions (median [IQR], 1.47 [1.38–1.55] seconds), although statistical significance was not reached (*P* = 0.066). Similarly, comparing ISUP group ≥2 PCa to ISUP group 1 PCa and benign prostate lesions, no statistically significant difference in T1 relaxation time was evident (*P* = 0.123).

TABLE 2 - T1 Relaxation Time (s) and ADC Values (s/mm^2) of Radiologically Identified Prostate Lesions According to ISUP Groups

Parameter	Level	ISUP Group 1	ISUP Group 2	ISUP Group 3	ISUP Group 4	Benign
n		3	15	3	1	49
T1 relaxation time	Median (IQR)	1.33 (1.33–1.41)	1.41 (1.37–1.47)	1.29 (1.25–1.37)	1.4 (1.4–1.4)	1.47 (1.38–1.55)
ADC value	Median (IQR)	0.836 (0.792–0.899)	0.789 (0.738–0.882)	0.896 (0.736–0.964)	0.781 (0.781–0.781)	0.884 (0.799–0.965)

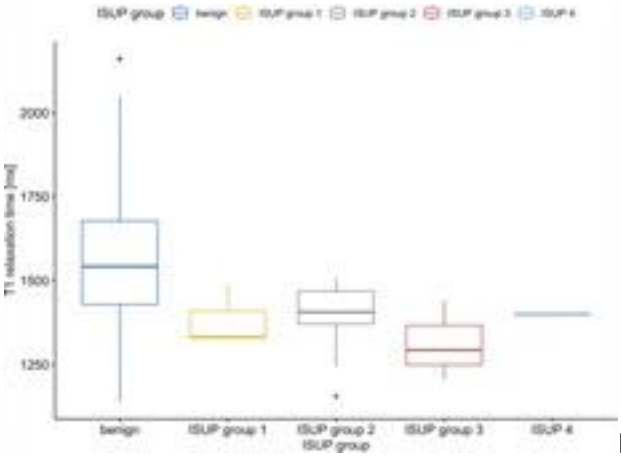

FIGURE 4:
T1 relaxation times (milliseconds) of prostate lesions according to histological grading.

Diagnostic Performance of T1 Relaxation Time and ADC Values

For discrimination of PCa from reference regions in the PZ and TZ (including BPH nodules) as well as radiologically suspicious prostate lesions with benign histology, T1 relaxation times demonstrated an AUC (IQR) = 0.8 (0.72–0.87), whereas ADC values showed an AUC (IQR) = 0.83 (0.76–0.9; *P* = 0.519). Using the Youden index for definition of optimal cutoff, T1 relaxation times yielded a sensitivity = 0.59 and specificity = 1, and ADC values a sensitivity = 0.59 and specificity = 1. The corresponding ROC curves are depicted in Figure 5.

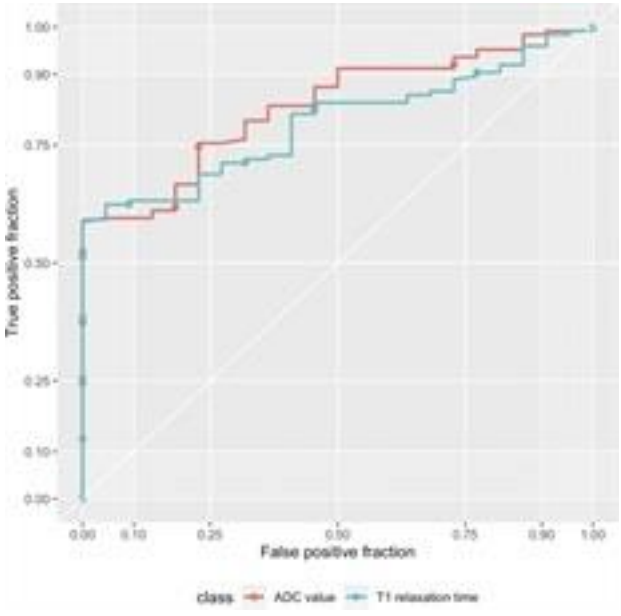

FIGURE 5:
ROC curves of T1 relaxation time and ADC value for discrimination of PCA versus reference regions in the peripheral and transitional zone, BPH nodules as well as radiologically suspicious prostate lesions with benign histology.

Discriminating PCa from radiologically suspicious prostate lesions with benign histology, T1 relaxation times showed an AUC (IQR) = 0.69 (0.57–0.81), and ADC values showed an AUC (IQR) = 0.62 (0.47–0.77; *P* = 0.446). Using the Youden index, T1 relaxation times yielded a sensitivity = 0.47 and specificity = 1, and ADC values yielded a sensitivity = 0.8 and specificity = 0.5. Corresponding ROC curves are provided in Figure 6.

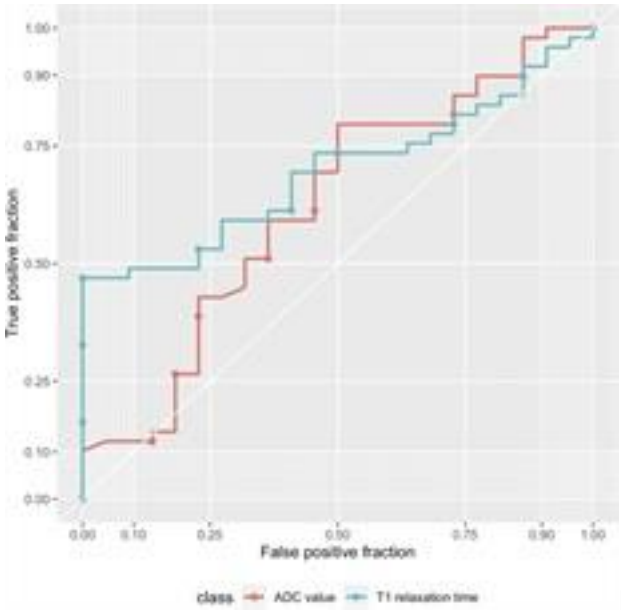

FIGURE 6:
ROC curves of T1 relaxation time and ADC value for discrimination of PCA versus radiologically suspicious prostate lesions with benign histology.

DISCUSSION

Prostate cancer identification and classification on mpMRI is an ongoing radiological challenge, as reflected by its current low specificity using PI-RADS assessment.[5] This study reports the clinical feasibility and utility of the T1FLASH technique for prostate assessment by T1 mapping. Prospectively enrolling 67 participants with suspicion of csPCa, our results demonstrate that T1FLASH-based T1 mapping is implementable in a clinical routine setting. T1FLASH T1 maps at 3.8 seconds measuring time per slice offer a robust quantification of prostate tissue properties without evident image artifacts, whereas quickly covering the prostate volume at an average examination time of 2:10 minutes for a stack of at least 30 maps.

In general, T1 relaxation times varied according to prostatic tissue type, with longest times evident in the PZ, whereas PCa lesions demonstrated the shortest T1 relaxation time (overall difference $P < 0.001$). For both the TZ and the PZ, PCa lesions showed shorter T1 relaxation times when compared with respective reference regions ($P < 0.05$, each). This translated into an AUC = 0.8 for discrimination of lesions from reference regions and radiologically suspicious lesions with benign histology, which was comparable to that of ADC values (AUC = 0.83, $P = 0.519$).

Comparing T1 relaxation times across ISUP groups, there was a tendency toward shorter times with increasing PCa grade, although statistical significance was not reached ($P = 0.066$), which might be attributable to the low number of included PCa lesions. This resulted in a numerically higher AUC for T1 relaxation times, comparing PCa to radiologically suspicious prostate lesions with benign histology (AUC = 0.69), in contrast to ADC values (AUC = 0.62, $P = 0.446$). These results indicate that T1FLASH-based T1 mappingof the prostate might add diagnostic value for the radiological identification and discrimination of PCa prostate lesions. Given our data, T1 maps and ADC values could complement each other in a comprehensive approach to prostate MRI assessment, with DWI/ADC for visual PCa detection and T1FLASH for further ISUP characterization. Still, given the missing statistical significance in the here presented data, as of now there is no clear indication whether T1FLASH maps will improve PCa assessment over established mpMRI sequences. Therefore, T1FLASH mapping of the prostate needs to be further evaluated in large prospective patient cohorts with independent validation.

The T1FLASH technique presented here has so far been evaluated only for cardiac applications, and to the best of our knowledge, this study is the first to analyze the clinical feasibility and utility of T1FLASH for T1 mapping of the prostate.[16] The technical hallmark of this T1 mapping technique is the highly undersampled radial FLASH readout, which results in extremely short acquisition times of 3.8 seconds per slice. Despite its high temporal resolution, T1FLASH offers a robust and accurate measurement of T1 relaxation times, which has been validated in phantom studies.[16] In combination with innovative local means filters, the SNR of T1FLASH T1 maps is further optimized without introducing relevant blurring.[22] Clinically, these specific properties of T1FLASH T1 maps translate into a short acquisition time and robust image quality, which corroborates its clinical applicability.

Few other research groups have so far evaluated the utility of T1 mapping for PCa. For example, Baur et al[13]used a MOLLI sequence for assessment of the prostate in 23 patients using a 3 T MR scanner. The mean image acquisition time for MOLLI sequences was 4:28 minutes as compared with 2:10 minutes in our study. In line with our findings, the authors reported varying T1 relaxation times according to prostate regions, with longest times in the PZ. Still, no statistically significant difference in T1 relaxation time was evident comparing PCa ISUP groups (P = 0.31). Continuing patient accrual at Berlin Charité, Makowski et al[28] used radiomics and machine learning to evaluate 66 PCa patients with mpMRI and additional MOLLI T1 mapping. The authors reported a high diagnostic accuracy of AUC = 0.92 for discriminating PCa Gleason score, thus underlining the utility of MOLLI T1 mapping for PCa assessment. Foltz and colleagues[14] used a magnetization-prepared spiral imaging technique to assess T1 relaxations times in 13 PCa patients with a 1.5 T MR scanner. The authors described shorter T1 relaxation times of PCa compared with both the TZ and PZ (P= 0.031, P = 0.029, respectively). Recently, Yu et al[29] implemented a MR fingerprinting approach in 140 PCa patients, including T1 mapping using a steady-state free precession technique using a 3 T MR scanner. The image acquisition time for MR fingerprinting with combined T1 and T2 mapping was 7:30 minutes. Focusing on the PZ, the authors reported a shorter T1 relaxation time for PCa compared with reference PZ regions (P < 0.001). However, no statistically significant difference in T1 relaxation time across PCa grades was evident.

This study is not devoid of limitations. First, given its design as a clinical feasibility study, only few participants were included, which could have limited the statistical power to detect imaging parameter differences across subgroups, as well as its generalizability. In particular, the low number of PCa patients and ISUP groups might have prevented statistically significant results comparing T1 relaxation times across subgroups. The small study cohort also limits the application of novel analysis techniques, such as machine learning. Second, although T1FLASH T1 maps offer robust results at a short examination time, the iterative reconstruction approach necessitates a dedicated reconstruction PC, resulting in high initial investment costs for the local technical implementation. Third, the T1FLASH T1 mapping technique presented in this study was only tested on one high-end clinical 3 T scanner. Thus, further studies are needed to evaluate whether our results are reproducible on other MR scanners with lower magnetic field strength or gradients. Fourth, US/MRI fusion-guided biopsies might have missed their targeted mpMRI lesions as well as radiologically obscured PCa lesions. Although a MR-guided prostate biopsy approach might have improved accuracy of prostate sampling, this biopsy technique was beyond the technical limits of this trial given its design as a feasibility study. Further, the high number of prostate lesions identified in the TZ with low proportion of PCa (22%) might point toward a bias in radiological TZ lesion assessment on mpMRI. Finally, the diagnostic accuracy evaluated in this study depends on the correct radiological identification of prostate lesions on mpMRI and might therefore lack generalizability.

To address some of these limitations, our research group continues patient enrollment to increase the patient cohort and bolster statistical power. Moving further from a per-lesion to a per-patient analysis approach, deep learning algorithms will be used to provide a more robust and generalizable assessment of the additional diagnostic benefit of T1FLASH maps over established mpMRI sequences.

CONCLUSIONS

T1FLASH-based T1 mapping yields robust results for quantification of the prostate at a short examination time of 2:10 minutes without evident image artifacts. Associated quantifiable T1FLASH T1 relaxation times could aid in discrimination of significant and nonsignificant PCa. Additional studies are warranted to confirm these results in a larger patient cohort and to assess the additional benefit of T1FLASH maps in conjunction with mpMRI sequences in the setting of deep learning. Further, the robustness of T1FLASH maps compared with potentially artifact-prone DWI sequences needs to be clinically evaluated in prospective trials.

REFERENCES

1. Bray F, Ferlay J, Soerjomataram I, et al. Global cancer statistics 2018: GLOBOCAN estimates of incidence and mortality worldwide for 36 cancers in 185 countries. *CA Cancer J Clin*. 2018;68:394–424.
2. Bell KJ, Del Mar C, Wright G, et al. Prevalence of incidental prostate cancer: a systematic review of autopsy studies. *Int J Cancer*. 2015;137:1749–1757.
3. Kasivisvanathan V, Rannikko AS, Borghi M, et al. MRI-targeted or standard biopsy for prostate-cancer diagnosis. *N Engl J Med*. 2018;378:1767–1777.
4. Barentsz JO, Richenberg J, Clements R, et al. ESUR prostate MR guidelines 2012. *Eur Radiol*. 2012;22:746–757.
5. Drost FH, Osses DF, Nieboer D, et al. Prostate MRI, with or without MRI-targeted biopsy, and systematic biopsy for detecting prostate cancer. *Cochrane Database Syst Rev*. 2019;4:Cd012663.
6. Costa DN, Xi Y, Aziz M, et al. Prospective inclusion of apparent diffusion coefficients in multiparametric prostate MRIstructured reports: discrimination of clinically insignificant and significant cancers. *AJR Am J Roentgenol*. 2019;212:109–116.
7. Bischoff LM, Katemann C, Isaak A, et al. T2 Turbo spin echo with compressed sensing and propeller acquisition (sampling k-space by utilizing rotating blades) for fast and motion robust prostate MRI: comparison with conventional acquisition. *Invest Radiol*. 2022; Publish ahead of print.
8. Raczeck P, Frenzel F, Woerner T, et al. Noninferiority of monoparametric MRI versus multiparametric MRI for the detection of prostate cancer: diagnostic accuracy of ADC ratios based on advanced “zoomed” diffusion-weighted imaging. *Invest Radiol*. 2022;57:233–241.
9. Langbein BJ, Szczepankiewicz F, Westin CF, et al. A pilot study of multidimensional diffusion MRI for assessment of tissue heterogeneity in prostate cancer. *Invest Radiol*. 2021;56:845–853.
10. Winkel DJ, Tong A, Lou B, et al. A novel deep learning based computer-aided diagnosis system improves the accuracy and efficiency of radiologists in reading biparametric magnetic resonance images of the prostate: results of a multireader, multicase study. *Invest Radiol*. 2021;56:605–613.
11. Taylor AJ, Salerno M, Dharmakumar R, et al. T1 mapping: basic techniques and clinical applications. *JACC Cardiovasc Imaging*. 2016;9:67–81.
12. Child N, Suna G, Dabir D, et al. Comparison of MOLLI, shMOLLLI, and SASHA in discrimination between health and disease and relationship with histologically derived collagen volume fraction. *Eur Heart J Cardiovasc Imaging*. 2017;19:768–776.
13. Baur ADJ, Hansen CM, Rogasch J, et al. Evaluation of T1 relaxation time in prostate cancer and benign prostate tissue using a modified Look-Locker inversion recovery sequence. *Sci Rep*. 2020;10:3121.
14. Foltz WD, Haider MA, Chung P, et al. Prostate T(1) quantification using a magnetization-prepared spiral technique. *J Magn Reson Imaging*. 2011;33:474–481.
15. Wang X, Roeloffs V, Merboldt KD, et al. Single-shot multi-slice T1 mapping at high spatial resolution—inversion-recovery FLASH with radial undersampling and iterative reconstruction. *Open Med Imag J*. 2015;9:1–8.

16. Wang X, Joseph AA, Kalentev O, et al. High-resolution myocardial T(1) mapping using single-shot inversion recovery fast low-angle shot MRI with radial undersampling and iterative reconstruction. *Br J Radiol*. 2016;89:20160255.
17. Weinreb JC, Barentsz JO, Choyke PL. PI-RADS. Prostate Imaging–Reporting and Data System. 2019. Available at: https://www.acr.org/-/media/ACR/Files/RADS/Pi-RADS/PIRADS-V2-1.pdf. Accessed 29.12.2022.
18. Giganti F, Allen C, Emberton M, et al. Prostate imaging quality (PI-QUAL): a new quality control scoring system for multiparametric magnetic resonance imaging of the prostate from the PRECISION trial. *Eur Urol Oncol*. 2020;3:615–619.
19. Roeloffs V, Voit D, Frahm J. Spoiling without additional gradients: radial FLASH MRI with randomized radiofrequency phases. *Magn Reson Med*. 2016;75:2094–2099.
20. Voit D, Kalentev O, Frahm J. Body coil reference for inverse reconstructions of multi-coil data-the case for real-time MRI. *Quant Imaging Med Surg*. 2019;9:1815–1819.
21. Uecker M, Zhang S, Voit D, et al. Real-time MRI at a resolution of 20 ms. *NMR Biomed*. 2010;23:986–994.
22. Klosowski J, Frahm J. Image denoising for real-time MRI. *Magn Reson Med*. 2017;77:1340–1352.
23. Epstein JI, Egevad L, Amin MB, et al. The 2014 International Society of Urological Pathology (ISUP) consensus conference on Gleason grading of prostatic carcinoma: definition of grading patterns and proposal for a new grading system. *Am J Surg Pathol*. 2016;40:244–252.
24. Rosner B, Glynn RJ, Lee ML. Extension of the rank sum test for clustered data: two-group comparisons with group membership defined at the subunit level. *Biometrics*. 2006;62:1251–1259.
25. Datta S, Satten GA. A signed-rank test for clustered data. *Biometrics*. 2008;64:501–507.
26. Obuchowski NA. Nonparametric analysis of clustered ROC curve data. *Biometrics*. 1997;53:567–578.
27. Youden WJ. Index for rating diagnostic tests. *Cancer*. 1950;3:32–35.
28. Makowski MR, Bressem KK, Franz L, et al. De novo radiomics approach using image augmentation and features from T1 mapping to predict Gleason scores in prostate cancer. *Invest Radiol*. 2021;56:661–668.
29. Yu AC, Badve C, Ponsky LE, et al. Development of a combined MR fingerprinting and diffusion examination for prostate cancer. *Radiology*. 2017;283:729–738.